On the Polarization Diversity Performance of Log.-Per. Multiarm-Antennas for MB-OFDM UWB Communications

Oliver Klemp[a], Gunnar Armbrecht and Hermann Eul

[a]Universität Hannover, Institut für Hochfrequenztechnik und Funksysteme,
Hannover, Germany, e-mail: klemp@hft.uni-hannover.de

Abstract - The implementation of multiband OFDM ultra wideband (MB-OFDM UWB) technology into wireless devices is well suited in order to enhance transmission capacities for low-range wireless communications systems. According to the frequency allocation of the multiband OFDM alliance, UWB communications is planned in the frequency range from 3.1-10.6 GHz incorporating four groups of 13 frequency bands with an operational bandwidth of 528 MHz bandwidth each. Although OFDM transmission provides a certain robustness against multipath interference, signal fading may occur due to de-polarization effects introduced by the transmission channel. Polarization fading mitigation can be efficiently exploited using dual-polarized antenna elements that prevent from miss-alignment of TX- and RX- antennas as well as from de-polarization due to multipath propagation. Provided those antenna elements can be realized as compact and planar air interfaces with a small transversal extent, antenna elements of that kind are well suited to allow polarization-diversity operations for MB-OFDM terminals.

1 Introduction

UWB short-range wireless communications systems based on the technology of multiband OFDM (MB-OFDM) within the standards of IEEE 802.15.3 and IEEE 802.15.4 are about to become a global standard for short-range wireless multimedia networking in the frequency range from 3.1-10.6 GHz. In order to provide ubiquitous wireless connectivity, high-performance compact and light-weight antenna equipment is an integral part for the successful establishment of UWB MB-OFDM networks. For an effective polarization fading mitigation [1], [2], antennas are to be used that offer polarization-invariant transmission characteristics. Diversity concepts as in [1], [3], [4] at the receiver may be then used in order to enhance the signal-to-noise ratio (SNR) in fading environments without increasing signal power. Applying usual diversity combination techniques at the receiver, high diversity gains could be achieved over a wide frequency band.
Suitable antenna elements that are able to cover the whole frequency band of operation are a key parameter in the successful implementation of UWB communication systems. Especially for UWB communications systems, antenna parameters like input impedance, antenna gain and radiation pattern need to be almost constant with frequency to provide identical transmission conditions for the whole frequency band of operation [5]. Self-complementary [6], logarithmically-periodic antennas serve as suitable representatives for the realization of broadband antenna structures. As shown in [7] they can be favorably used in polarization diverse transmission systems provided they adhere to a specific geometric structure.
The article is organized as follows: In Section 2 geometry and radiation parameters for a planar, dual-polarized, log.-per. trapezoid antenna for UWB-communications is reviewed. In order to derive the polarization diversity performance of the antenna element in a multipath-conditioned

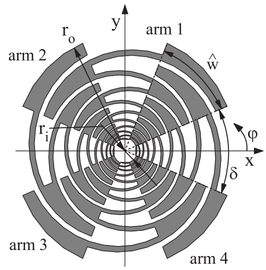

Figure 1: Geometry of polarization-diversity UWB trapezoid antenna in free-space.

Table 1: Geometry parameters of UWB trapezoid antenna in free space.

parameter	δ / °	$\hat{w}$ / °	r_{i} / mm	r_{o} / mm
value	45	45	2	30

environment, Section 3 derives a narrow-band stochastic model of the communications channel that accounts for polarization fading. The results of polarization diversity performance presumed a maximum ratio combining at the receiver are summarized in Section 4, Section 5 concludes the article.

2 Dual Polarized MB-OFDM Broadband Antenna Design

For the design of compact antenna structures with dual-polarized radiation patterns, log.-per. four-arm antennas as considered in [7] can be easily integrated into dual-polarized short-range wireless communication devices. Due to the availability of four electromagnetically decoupled antenna arms, elements of that kind offer two almost orthogonal port-related far-field patterns that result from the odd-phase excitation of two adjacent antenna arms. Provided the antenna elements adhere to the principle of self-complement they theoretically show a frequency-independent real input impedance of $133\,\Omega$ at the individual antenna ports [8] in free-space.
Fig. 1 depicts the dual-polarized four-arm trapezoid UWB antenna that is used for polarization diversity analysis in the UWB frequency band according to the design considerations given in [9]. The geometry parameters for the antenna element in free-space are summarized in Table 1. The frequency independence of antenna radiation behavior can be viewed from Fig. 2 a) and Fig. 2 b) and c) representing normalized antenna far-field patterns at 3.0 GHz and 11.0 GHz. Excellent far-field decoupling of the two port-related antenna radiation patterns can be viewed from the cross polarization suppression in antenna main beam direction, $\Gamma\left(\vartheta_0 = 0°, \varphi_0 = 0°\right)$. This quantity relates the co-polar electrical field strength to the cross-polar electrical field strength of one distinct antenna operational mode in antenna main beam direction. The trapezoidal four-arm antenna design provides an outstanding degree of cross polarization discrimination in main beam direction in the order of 20 dB in the entire frequency range of operation as can be seen from Fig. 2 a).

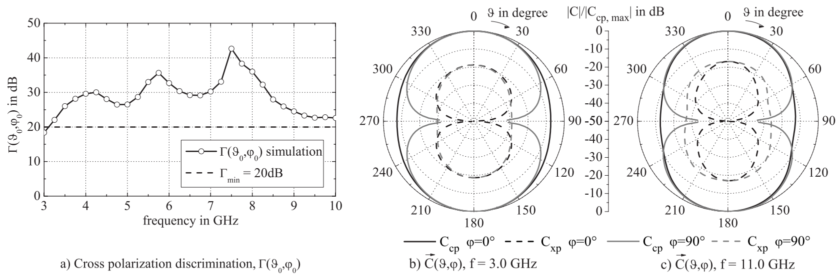

Figure 2: Simulated results for cross-polarization discrimination $\Gamma(\vartheta_0, \varphi_0)$ and radiation patterns $\vec{C}(\vartheta, \varphi)$ of UWB antenna design in free-space.

3 Channel Model for Polarization Diversity Reception

In terms of diversity combination, the model of the radio channel is used as given in Fig. 3. Due to the two-branch reception of incoming waves at the receiver, $r_1(t)$ and $r_2(t)$ denote the signal envelopes that are related to the two operational modes of the antenna geometry that yield dual-linear polarization. The related antenna radiation patterns of the two operational modes are given by $\vec{C}_1(\vartheta, \varphi)$ and $\vec{C}_2(\vartheta, \varphi)$. For signal-to-noise- (SNR-) analysis, additive white Gaussian noise is introduced at both diversity branches by $n_1(t)$ and $n_2(t)$. Diversity combining of the branch envelopes results in the output envelope $\tilde{r}(t)$. Corresponding branch weights α_1 and α_2 are properly chosen according to the signal-to-noise ratios of the respective diversity branches in order to perform maximum ratio combining [4]. For the generation of correlated radio signals a simple model is applied that accounts for the spatial correlation properties at the receiver. Antenna correlation is determined from the radiation patterns of the diversity antenna in the two distinct operational modes. The resulting signal correlation matrix is used for a transformation of uncorrelated complex Gaussian radio signals into correlated Rayleigh envelope processes according to [10]. A Cholesky factorization of the computed correlation matrix $\mathbf{R}^{\mathrm{RX}}$ yields $\mathbf{R}^{\mathrm{RX}} = \mathbf{L}^{\mathrm{RX}} \mathbf{L}^{\mathrm{RX}^H}$, where $\mathbf{L}^{\mathrm{RX}}$ denotes the lower triangular matrix of $\mathbf{R}^{\mathrm{RX}}$. In order to simulate Rayleigh envelope fading behavior, each diversity branch $i = 1, 2$ is modeled via an uncorrelated complex Gaussian time sequence $\mathbf{w}$. The vector of correlated Gaussian time

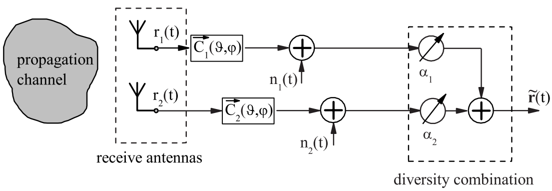

Figure 3: Model of receiver structure applying co-located, dual-polarized antenna elements and subsequent diversity combination.

sequences $\mathbf{x}$ and corresponding Rayleigh envelopes $\mathbf{r} = |\mathbf{x}|$ can be directly computed from matrix transformation $\mathbf{x} = \mathbf{L}^{\mathrm{RX}}\mathbf{w}$ involving the vector of uncorrelated Gaussian time sequences $\mathbf{w}$. The complex correlation coefficient $\rho_{\mathrm{i,j}}$ between antenna operational modes i and j at the receiver is given by $\rho_{\mathrm{i,j}} = R_{\mathrm{i,j}}/\sqrt{\sigma_{\mathrm{i}}^2\sigma_{\mathrm{j}}^2}$ with $\{i,j\} = 1,2$, where R and σ represent antenna covariance- and variance. For the regarded polarization diversity antenna offering $n = 2$ diversity branches, respective correlation coefficients can be combined to the desired spatial correlation matrix $\mathbf{R}^{\mathrm{RX}}$ as given in (1).

$$\mathbf{R}^{\mathrm{RX}} = \begin{bmatrix} \rho_{11}^{\mathrm{RX}} & \rho_{12}^{\mathrm{RX}} \\ \rho_{21}^{\mathrm{RX}} & \rho_{22}^{\mathrm{RX}} \end{bmatrix} \tag{1}$$

The off-diagonal values of $\mathbf{R}^{\mathrm{RX}}$ spot the correlation properties at the diversity antenna between different operational modes and the diagonal values amount to $\rho_{11}^{\mathrm{RX}} = \rho_{22}^{\mathrm{RX}} = 1$. In general, branch correlation and diversity performance depend on the distinct channel situation where the antenna is operated in. In this paper a simple model for the spatial properties of incoming waves at the receiver is applied, involving a stochastic formulation of the angle-of-arrival (AoA) situation which is given by a two-dimensional probability density $p_{\vartheta,\varphi}(\vartheta,\varphi)$ according to [11]. The probability density is defined in the entire interval of elevation $0 \leq \vartheta \leq \pi$ and azimuth $0 \leq \varphi \leq 2\pi$ and applies for both antenna polarizations in the directions of ϑ and φ. Antenna covariance $R_{\mathrm{i,j}}$ can be computed from:

$$\begin{aligned} R_{\mathrm{i,j}} &= \mathrm{K}_0 \int_0^{2\pi}\int_0^{\pi} \left[\mathrm{XPD}\, C_{\varphi,\mathrm{i}}(\vartheta,\varphi)\, C_{\varphi,\mathrm{j}}^{*}(\vartheta,\varphi)\right. \\ &+ \left. C_{\vartheta,\mathrm{i}}(\vartheta,\varphi)\, C_{\vartheta,\mathrm{j}}^{*}(\vartheta,\varphi)\right] e^{j\vec{k}\vec{r}_{ij}} p_{\vartheta,\varphi}(\vartheta,\varphi) \sin\vartheta d\vartheta d\varphi\,. \end{aligned} \tag{2}$$

In (2), XPD denotes the cross-polarization suppression inherent to the multipath communication channel and K_0 stands for a proportionality constant. Subsequently, the ideal case for polarization diversity combining with $\mathrm{XPD} = 1$ is considered. Variances σ_i^2 can be computed from (2) replacing $i = j$. In order to determine the diversity performance of the broadband dual-polarized antenna structure, Monte-Carlo simulations are carried out, involving $N_{\mathbf{w}} = 10000$ realizations of Rayleigh fading coefficients $\mathbf{w}$. The fading process is assumed to provide uncorrelated zero-mean complex Gaussian variables with a unit variance. In Section 4, the described signal model is applied to the investigation of polarization diversity performance of the wideband antenna.

4 Polarization Diversity Analysis

Diversity performance of the optimized trapezoid antenna as given in Section 2 is derived from maximum ratio combining (MRC) [4] in a frequency range from 3 GHz to 11 GHz. The spatial properties of the regarded channel scenario $p_{\vartheta,\varphi}(\vartheta,\varphi)$ are modeled by a Laplacian density in azimuth and a Gaussian density in elevation in accordance to [12]. Mean values of the AoA behavior are given by $m_\vartheta = 90°$ and $m_\varphi = 90°$ for an antenna element centered in the xz-plane of the respective cartesian coordinate system. Due to a high degree of cross polarization decoupling, branch power correlation $|\rho_{1,2}|^2 = |\rho_{2,1}|^2$ remains below 0.05 in the considered channel scenario at all operational frequencies and is therefore not plotted here explicitly. The angular spreads are assumed as $\sigma_\vartheta = 20°$ in elevation and $\sigma_\varphi = 60°$ in azimuth. Diversity gains $G_{\mathrm{MRC,P}}$ at the probability level P will be computed by a comparison of the signal-to-noise ratios Γ_{c} of the combined output signal $\tilde{r}$ and the signal-to-noise ratio $\gamma_{\max}$ of the branch with the best signal-to-noise behavior before diversity combining.
Fig. 4 a) represents simulation results from Monte Carlo analysis of polarization diversity performance for the antenna module at 7 GHz. The cumulative distribution functions (CDFs) are

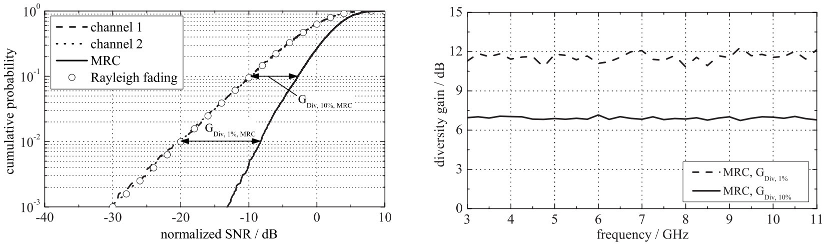

a) CDF for maximum ratio combining at 7.0 GHz

b) Frequency dependence of diversity gain

Figure 4: Results of polarization diversity performance for the UWB trapezoid antenna using maximum ratio combining.

normalized with respect to the time average of the stronger diversity branch in accordance to [4]. As a result from the low values of diversity branch correlation, the CDFs tend to converge to the uncorrelated Rayleigh curve. At the distinct levels with a cumulative probability of $P = 1\%$, the respective diversity gain amounts to $G_{\mathrm{MRC},1\%} = 12.1\,\mathrm{dB}$. A cumulative probability limit of 10% results in a diversity gain of $G_{\mathrm{MRC},10\%} = 6.8\,\mathrm{dB}$. The results for broadband polarization diversity performance in the entire frequency band of operation from 3.0 GHz to 11.0 GHz are given in Fig. 4 b) for cumulative probability levels of 1% and 10%. The results offer frequency-independent values of diversity gain. Due to the frequency-independent behavior of antenna radiation patterns and cross-polarization discrimination, the use of polarization diversity combination is therefore well suited in order to suppress polarization fading at all operational frequencies of the antenna. Performing a stochastic investigation of the frequency dependence of diversity gain, the mean values $m_{\mathrm{MRC,\,P}}$ and standard deviations $\sigma_{\mathrm{MRC,\,P}}$ are derived from the processes of diversity gain as given in Fig. 4 b). At a cumulative probability level of 1%, maximum ratio combining yields a mean value of $m_{\mathrm{MRC,\,1\%}} = 11.6\,\mathrm{dB}$ and a small standard deviation of $\sigma_{\mathrm{MRC,\,1\%}} = 0.4\,\mathrm{dB}$. For an enhanced cumulative probability of 10%, a mean diversity gain of 6.9 dB and a respective standard deviation of 0.1 dB are computed.

5 Conclusion

In this paper, the self-complementary, log.-per. four-arm trapezoid antenna was investigated to cover the frequency range from 3.1 GHz to 10.6 GHz for polarization diversity reception. A simple stochastic model of the multipath communication channel was applied in order to derive the polarization diversity performance of the antenna in this frequency range. Due to its excellent cross-polarization decoupling in the whole frequency band of operation, polarization diversity reception and subsequent maximum ratio combining yields a high diversity gain with a mean value of 6.9 dB and a small variance of 0.1 dB at a cumulative probability level of 10%. For that reason, the four-arm trapezoid UWB antenna may be favorably used for the integration into compact UWB communications systems applying polarization diversity reception.

References

[1] R. G. Vaughan, "Polarization diversity in mobile communications," *IEEE Transactions on Vehicular Technology*, vol. 39, pp. 177–186, 2004.

[2] K. Y. Yazdandoost and R. Ohno, "Low-profile, dual-polarized broadband antennas," *Antennas and Propagation Society International Symposium*, vol. 2, pp. 256–259, 2003.

[3] W. C.-Y. Lee and Y. S. Yeh, "Polarization diversity system for mobile radio," *IEEE Trans. Commun.*, vol. COM-20, pp. 912–923, 1972.

[4] K. Dietze, C. B. Dietrich, and W. L. Stutzman, "Analysis of a two-branch maximal ratio and selection diversity system with unequal SNRs and correlated inputs for a rayleigh fading channel," *IEEE Transactions on Wireless Communications*, vol. 1, pp. 274–281, 2002.

[5] K. Y. Yazdandoost and R. Ohno, "Ultra wideband antenna," *IEEE Communications Magazine*, vol. 42, pp. 29–32, 2004.

[6] R. H. DuHamel and D. E. Isbell, "Broadband logarithmically periodic antenna structures," *IRE International Convention Record*, vol. 5, pp. 119–128, 1957.

[7] O. Klemp, M. Schultz, and H. Eul, "Novel logarithmically periodic antenna structures for broadband polarization diversity reception," *AEUE, International Journal on Electronics and Communications*, vol. 59, pp. 268–277, 2005.

[8] G. A. Deschamps, "Impedance properties of complementary multiterminal planar structures," *IRE Transactions on Antennas and Propagation*, vol. AP-7, pp. 371–378, 1959.

[9] O. Klemp and H. Eul, "Design of compact logarithmically periodic antenna structures for polarization-invariant UWB communication," *Proceedings of the* 2^{nd} *Workshop on Positioning, Navigation and Communication and* 1^{st} *Ultra-Wideband Expert Talk, Hannover, Germany*, vol. 1, 16-17 March 2005.

[10] S. Sorooshyari and D. G. Daut, "Generation of correlated rayleigh fading envelopes for accurate performance analysis of diversity systems," *14th IEEE 2003 International Symposium on Personal, Indoor and Mobile Radio Communications*, vol. 1, pp. 1800–1804, 2003.

[11] T. Taga, "Analysis for mean effective gain of mobile antennas in land mobile radio environments," *IEEE Trans. Veh. Technol.*, vol. 39, pp. 117–131, 1990.

[12] C. Waldschmidt and W. Wiesbeck, "Compact wide-band multimode antennas for MIMO and diversity," *IEEE Transactions on Antennas and Propagation*, vol. 52, pp. 1963–1969, 2004.